Title

Demonstration of electronic pattern switching and 10x pattern demagnification in a maskless micro-ion beam reduction lithography system

Permalink

https://escholarship.org/uc/item/91f8x9r8

Authors

Ngo, V.V.
Akker, B.
Leung, K.N.
et al.

Publication Date

2002-05-31

Demonstrations of Electronic Pattern Switching and 10x Pattern Demagnification in a Maskless Micro-Ion Beam Reduction Lithography System[*]

V. V. Ngo[a,b], B. Akker, K. N. Leung[a], Isaac Noh, K. L. Scott[c], and S. Wilde
Lawrence Berkeley National Laboratory, 1 Cyclotron Rd., MS 5-121, CA 94720

Abstract

A proof-of-principle ion projection lithography (IPL) system called Maskless Micro-ion-beam Reduction Lithography (MMRL) has been developed and tested at the Lawrence Berkeley National Laboratory (LBNL) for future integrated circuits (ICs) manufacturing and thin film media patterning [1]. This MMRL system is aimed at completely eliminating the first stage of the conventional IPL system [2] that contains the complicated beam optics design in front of the stencil mask and the mask itself. It consists of a multicusp RF plasma generator, a multi-beamlet pattern generator, and an all-electrostatic ion optical column.

Results from ion beam exposures on PMMA and Shipley UVII-HS resists using 75 keV H+ are presented in this paper. Proof-of-principle electronic pattern switching together with 10x reduction ion optics (using a pattern generator made of nine 50-μm switchable apertures) has been performed and is reported in this paper. In addition, the fabrication of a micro-fabricated pattern generator [3] on an SOI membrane is also presented.

1. INTRODUCTION

The key active element in the lithographic step is the radiation, which serves as media for the pattern transfer, be it in the form of photon, electrons, or ions. Among the next generation technologies being explored, ion projection lithography (IPL) seems to be an effective and viable choice. Ions are particularly well suited for use in projection systems aimed at small minimum dimensions and high throughput IC production because they are, in effect, diffraction-free and suffer little scattering in the resist. In addition, the linewidth formed by ions on resist is not a

---

[*] This work is supported by DARPA and the US Department of Energy under contract number DE-AC03-76SF00099.

a) Also with the Department of Nuclear Engineering, University of California at Berkeley.
b) Email: csvvngo@nuc.berkeley.edu
c) Department of Electrical Engineering and Computer Science, University of California at Berkeley.

strong function of exposure dose and the resist sensitivity is independent of resist thickness or ion energy [5]. Figure 1(a) schematically shows a conventional ion projection systems in which a uniform divergent beam of light ions, H^+, H_2^+, or He^+, is accelerated to 10 keV and made parallel before impinging on a stencil mask. The stencil mask is a very thin membrane (~3 μm thick) with open holes for beam passage. After exiting the stencil mask, the beam is further accelerated to energies in 70-150 keV range and then demagnified (up to 8.4 x) into a parallel beam whose image is focused at the wafer. Projection systems like those built by IMS in Vienna, Austria have achieved minimum dimensions down to 65 nm with field distortion of less than 0.15 μm over an 8x8 mm area and have demonstrated many features needed for high throughput lithography [2]. However, there still exist issues involving the much complicated and expensive mask technology of this IPL approach.

Alternatively, a novel lithographic approach could be devised to have the high resolution and throughput of a projection system like the IPL system while possessing essential characteristics of a maskless system. That is, an ion projection lithography system which does not involve the mask changing process. Maskless Micro-ion-beam Reduction Lithography (MMRL), potentially is one such system. Figure 1(b) shows the schematics of this new approach. The MMRL scheme is proposed to completely eliminate the first stage of the conventional IPL system that contains the complicated beam optics design in front of the stencil mask and the mask itself. The main components of the MMRL system consist of a multicusp plasma generator, a multi-beamlet extraction system, and an accelerator column for beam reduction. These main components are the distinguishing features that set MMRL apart from its conventional IPL counter-part. As such, they are to be characterized using the performance requirement of current IPL systems as benchmarks.

2. EXPERIMENTAL SET-UP

Figure 2 shows a cut-away 3-D model of the integrated Maskless Micro-ion-beam Reduction Lithography (MMRL) system. Other peripheral components not shown in Fig. 2

include high-voltage power supplies, a high-voltage power isolation transformer, an (Radio Frequency) RF-power generator, an impedance matching network for the RF-power generator, a vacuum pump system, a control and automation system (Fig. 3), and the clean-room facility which houses the MMRL system at the Lawrence Berkeley National Laboratory.

3. RESULTS

3.1 Multi-cusp Plasma Ion Source

The RF-driven multi-cusp plasma ion source (Fig. 4) is capable of generating almost pure H^+ ions from a uniform plasma region with a diameter of nearly 20 cm (Fig. 4d). This allows for a very large area of a patterns (object field) to be illuminated. The characteristic cusp B-field configuration around the source chamber is generated by samarium-cobalt permanent magnet columns arranged with alternating polarity (Fig. 4a). The multi-cusp magnetic field provides efficient plasma confinement. The plasma is inductively heated by a 13.56 MHz radio frequency (RF) power generator.

The multi-cusp plasma ion source has been chosen for the MMRL system and for Ion Projection Lithography (IPL) applications in general because it can produce large volumes of uniform and quiescent plasma of H^+ ions (or even heavier gas species such as Ar) in which the energy spreads among the constituent ions or electrons of the extracted beam are of order or less than 1 eV (Fig. 4c) using a quartz (RF) antenna and a magnetic filter (Fig. 4b). The magnetic filter, with the adequate field strength, effectively separates the plasma chamber into a discharge region and an extraction region. By preventing ionizing electrons at the discharge side from crossing over to the extraction side, the magnetic filter defines an extraction region of ions with low energy spread. The low energy spread results in significant improvement in the chromatic blur of the projection system.

3.2 Electronic Pattern Generator

The pattern generator, consisting of an array of micro-apertures, is patterned on two (plasma and extraction) electrodes separated by a ~5-μm layer of insulating material (Fig. 5).

Individual ion beamlets can be switched on or off to form the lithographic pattern by biasing the extraction electrode with respect to the plasma electrode. Removing the use of stencil masks from the lithographic process via such an electronic pattern would result in enormous cost savings by eliminating the technology efforts for mask development, defect detection, and defect correction. The use of an electronic pattern would also offer improved flexibility for rapid implementation of new designs and higher throughputs due to time savings from the elimination of multiple mask steps.

Micro-ion beam extraction (without demagnification optics) and switching through a multi-layer (conductor-insulator-conductor) array of nine 50-μm apertures has already been reported [7]. To demonstrate proof-of-principle electronic beam switching in concert with the MMRL 10x demagnification optics, a 9-hole switchable pattern generator was mechanically fabricated and tested. Figure 6 shows proof-of-principle beam switching and demagnification results. In addition, a micro-fabricated switchable pattern generator has been fabricated on a Silicon-on-insulator (SOI) substrate (Fig. 7). Switching beamlet apertures of 1 to 4 μm diameters were defined using 10x (demagnification) optical lithography and deep etched into Si and SiO_2. Testing as well as the fabrication of a beta version of this pattern generator is in progress.

3.3 10x Electrostatic Ion Optics

The H^+ ion beamlets emerging from the universal pattern generator, forming the desired lithographic pattern, are accelerated to 75 keV (kilo-electron-volt) through the accelerator column—an all-electrostatic ion optical lens assembly. The pattern is reduced in size by this all-electrostatic lens system before it is projected onto the wafer surface. Future needs for electrostatic beam deflection can be achieved by using dipole, quadrapole, or octopole electrodes. The ion optics has been characterized with respect to IMS's IPL system [6] for the prototype MMRL 10x-demagnification lens system using the MUNRO code (Fig. 8).

3.4 Test Exposures Using Highly-doped Silicon Patterned Membrane

Patterned membranes were put in place of an electronic pattern generator to act as stencil masks (Fig. 9) for exposure tests in the MMRL prototype system. These patterned membranes were (a) 50-70 mm thick highly-doped Si membrane with Ø ~ 9 μm aperture diameters and (b) 20 μm thick highly-doped Si membrane (courtesy of IBM Almaden) with Ø ~ 1.6 μm aperture diameters.

Figure 10 shows exposure results on Shipley UVII-HS [(a) and (b)] and PMMA [(c) and (d)] resists. These results have confirmed the 10x demagnification ion optics of the MMRL system and the 166 nm resolution achieved thus far. These exposures were performed using a pulsed RF-generated plasma in which the pulse-lengths, hence the exposure time, are from 100 to 300 ms.

SUMMARY:

The MMRL system has been proposed as a novel alternative to conventional IPL methods by eliminating the diverging beam optics and the fragile and costly mask of IPL systems by using and electronically switchable pattern generator. In this work, we have experimentally demonstrated that the MMRL multi-cusp plasma ion source can provide the low energy-spread and uniform plasma required for next generation lithography (NLG). Resolution of 166 nm has been demonstrated on resist using thick Si patterned membranes. In addition, pattern switching has been demonstrated with a mechanically fabricated 9-micro-ion-beam pattern. Finally, the microfabrication of a micro-aperture switchable pattern generator on an SOI substrate with 1 μm apertures has also been demonstrated.

[1] V. V. Ngo, W. Barletta, Y. Lee, K. N. Leung, and N. Zahir, *J. Vac. Sci. Technol.* B **17**, 6 (1999).

[2] G. Stengl et al., *J. Vac. Sci. Technol.* **19**, 1164 (Nov./Dec. 1981).

[3] K.L. Scott, T.-J. King, M.A. Lieberman, and K.-N. Leung, *J. Vac. Sci. Technol.* B 18, 6 (2000).

[4] John Canning, International SEMATECH, *Technology Trends*, September 2000,Cahners Business Information.

[5] [2] J. Melngailis, A. A. Mondelli, I. L. Berry III, and R. Mohondro, J. Vac. Sci. Technol. B **16**, 3 (1998).

[6] V. V. Ngo, K. N. Leung, *Proc. SPIE 3777*, 156 (1999).

[7] Y. Lee, W. A. Barletta, K.N. Leung, V.V. Ngo, P. Scott, M. Wilcox, N. Zahir, *Nuc. Instruments & Methods in Physics Research A* **47**, (2001).

List of Figures:

Fig. 1: Conventional Ion Projection Lithography (IPL) system using a thin stencil mask membrane (a) versus the proposed Maskless Micro-Beam Reduction Lithography (MMRL) system using a universal pattern generator to form the lithographic pattern (b).

Fig. 2: 3-D model of the prototype MMRL system (cut-away view).

Fig. 3: Control and automation in the MMRL system. The exposure process is controlled via the major components of the MMRL system, such as the Burleigh 3-axis precision stage, the RF power amplifier, and various other power supplies

Fig. 4: Multi-cusp plasma ion source characterization: (a) plasma confinement by magnetic cusp-field lines, (b) high-purity atomic hydrogen ion species, (c) low beam energy spread (< 2 eV), and (d) plasma density uniformity up to ~70% of source diameter.

Fig. 5: Cross sections of electronic pattern generator's arrays of switchable micro-aperture. Patterns are generated by biasing individual switching electrodes positively with respect to the beam-forming electrode.

Fig. 6: Proof of principle beam switching together with MMRL's 10x demagnification ion optics.

Fig. 7: Micro-fabricated switchable pattern generator deep etched in SOI substrate.

Fig. 8: Ion optics characterization of prototype MMRL system with respect to IMS's IPL system.

Fig. 9: Patterned membranes used in exposure tests: (a) 50-70 mm thick highly-doped Si membrane with Ø ~ 9 μm aperture diameters and (b) 20 μm thick highly-doped Si membrane (courtesy of IBM Almaden) with Ø ~ 1.6 μm aperture diameters.

Fig. 10: Test exposure results demonstrating 10x demagnification ion optics and 166 nm resolution on Shipley UVII-HS [(a) and (b)] and PMMA [(c) and (d)] resists.

Figure 1:

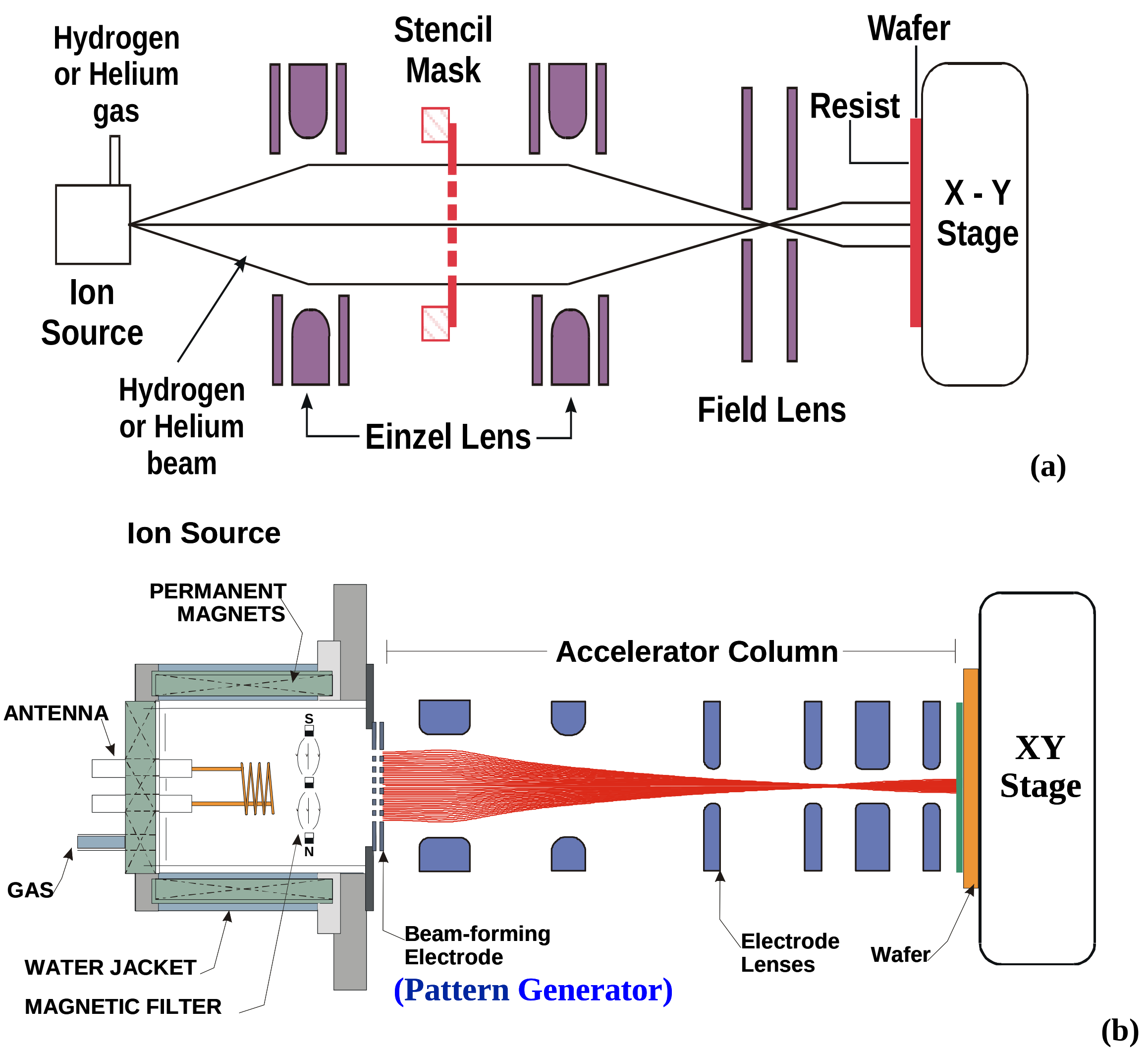

Figure 2:

Figure 3:

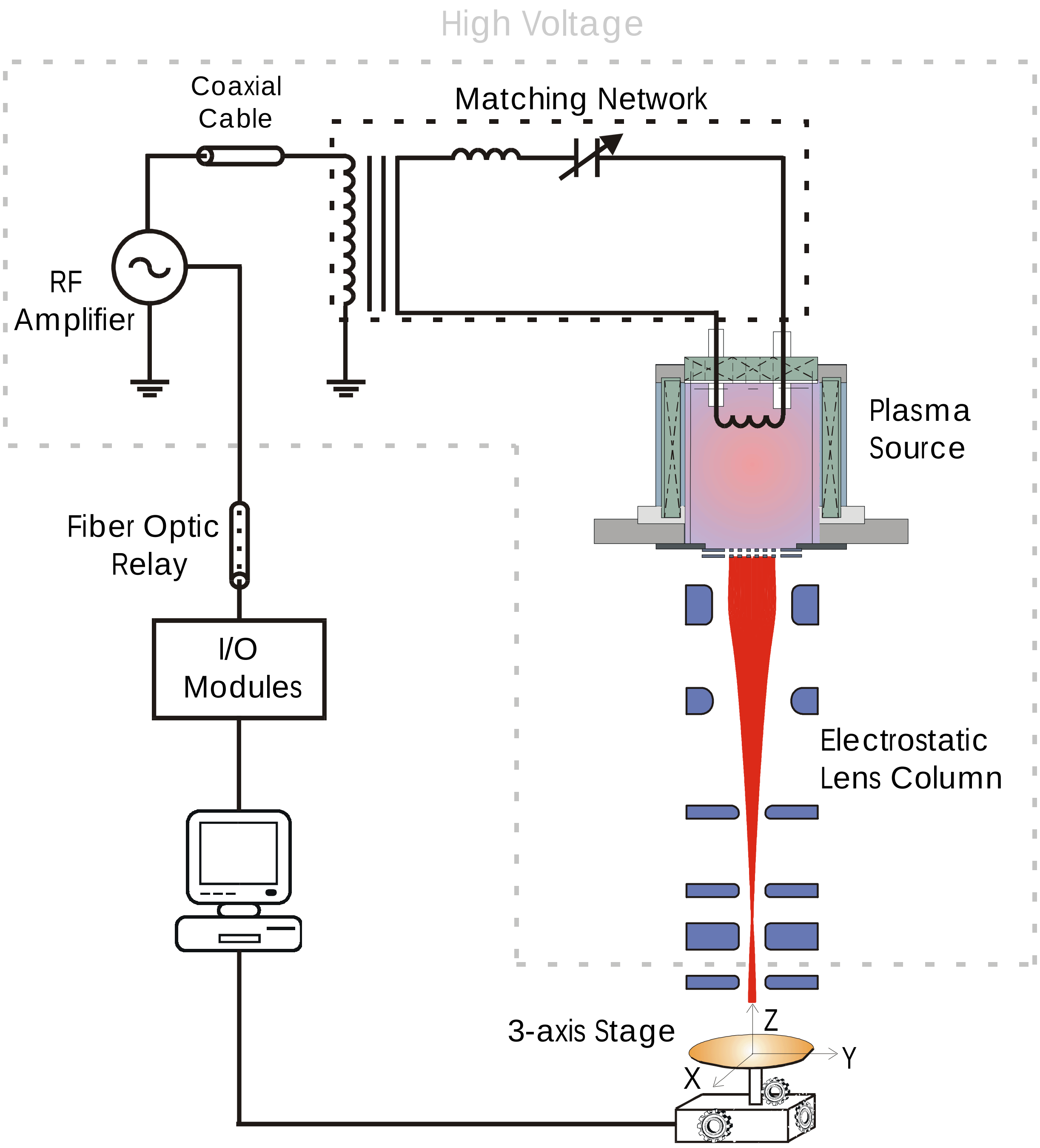
High Voltage
Coaxial Cable
Matching Network
RF Amplifier
Plasma Source
Fiber Optic Relay
I/O Modules
Electrostatic Lens Column
3-axis Stage
Z
Y
X

Figure 4:

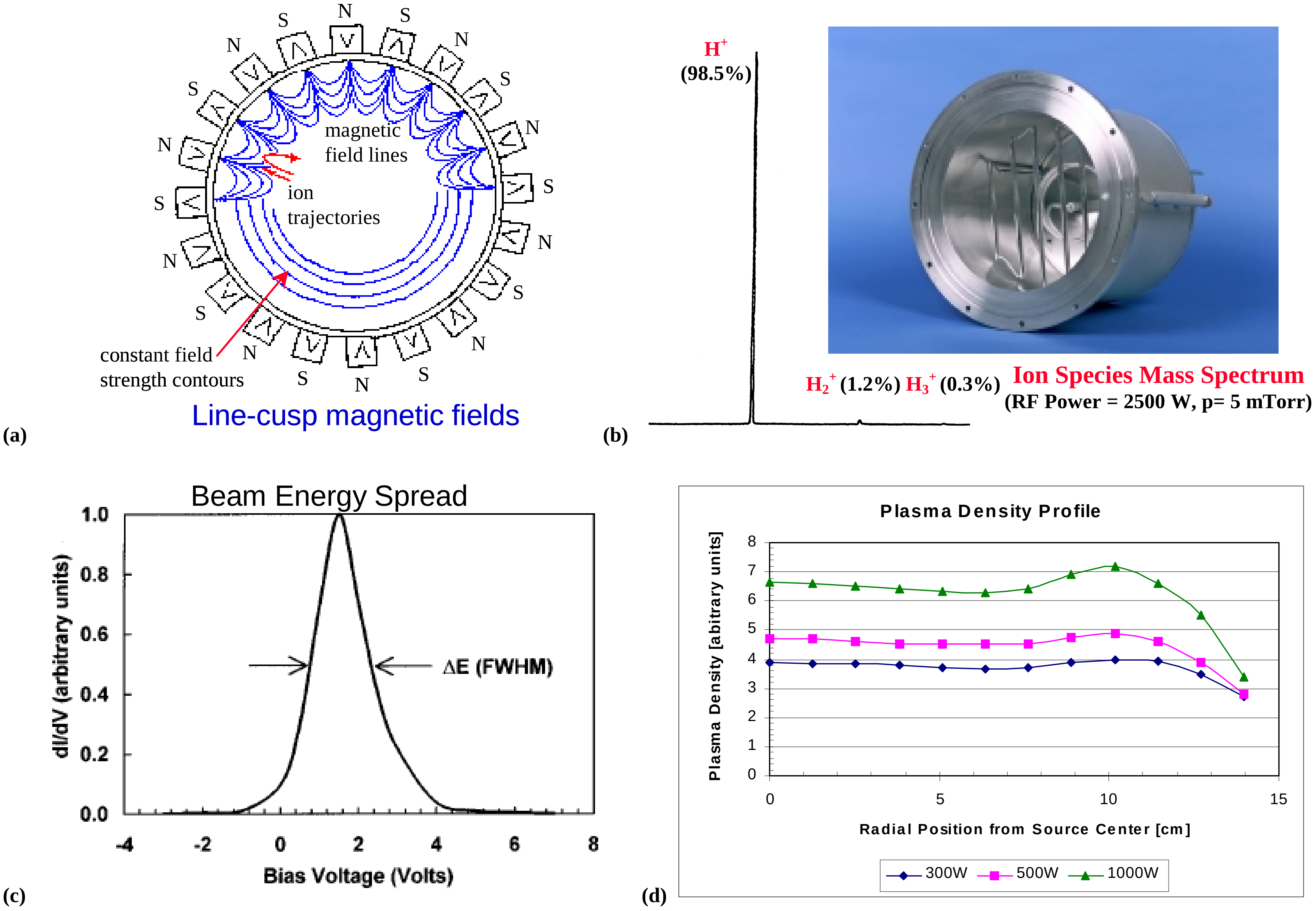
N
S
magnetic field lines
ion trajectories
constant field strength contours
Line-cusp magnetic fields
(a)
H^+ (98.5%)
H_2^+ (1.2%) H_3^+ (0.3%)
Ion Species Mass Spectrum
(RF Power = 2500 W, p= 5 mTorr)
(b)
Beam Energy Spread
dI/dV (arbitrary units)
1.0
0.8
0.6
0.4
0.2
0.0
ΔE (FWHM)
-4
-2
0
2
4
6
8
Bias Voltage (Volts)
(c)
Plasma Density Profile
Plasma Density [abitrary units]
8
7
6
5
4
3
2
1
0
0
5
10
15
Radial Position from Source Center [cm]
300W
500W
1000W
(d)

Figure 5:

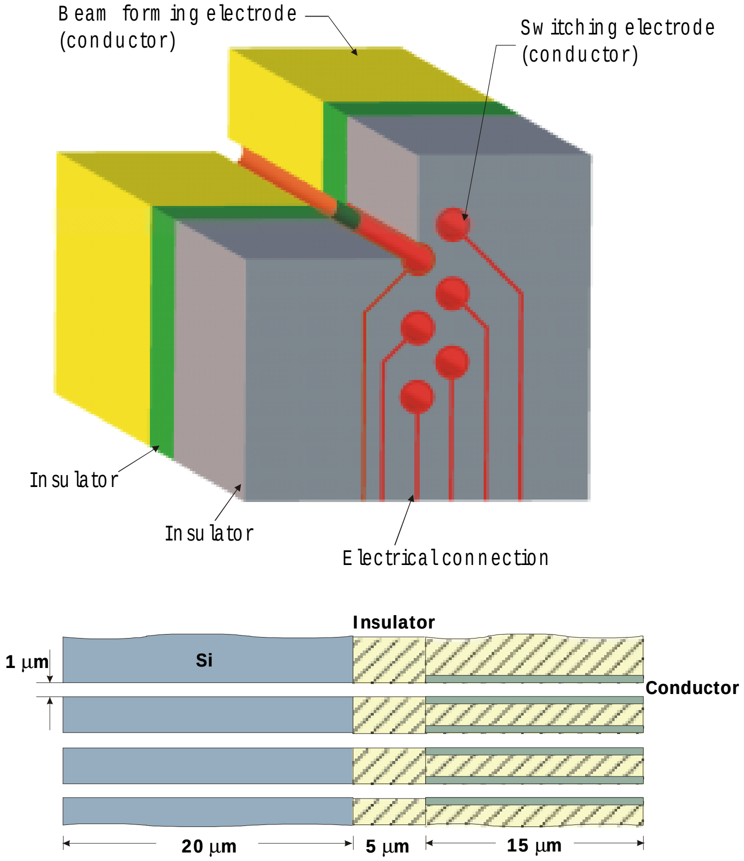
Beam forming electrode (conductor)
Switching electrode (conductor)
Insulator
Insulator
Electrical connection
Insulator
1 µm
Si
Conductor
20 µm
5 µm
15 µm

Figure 6:

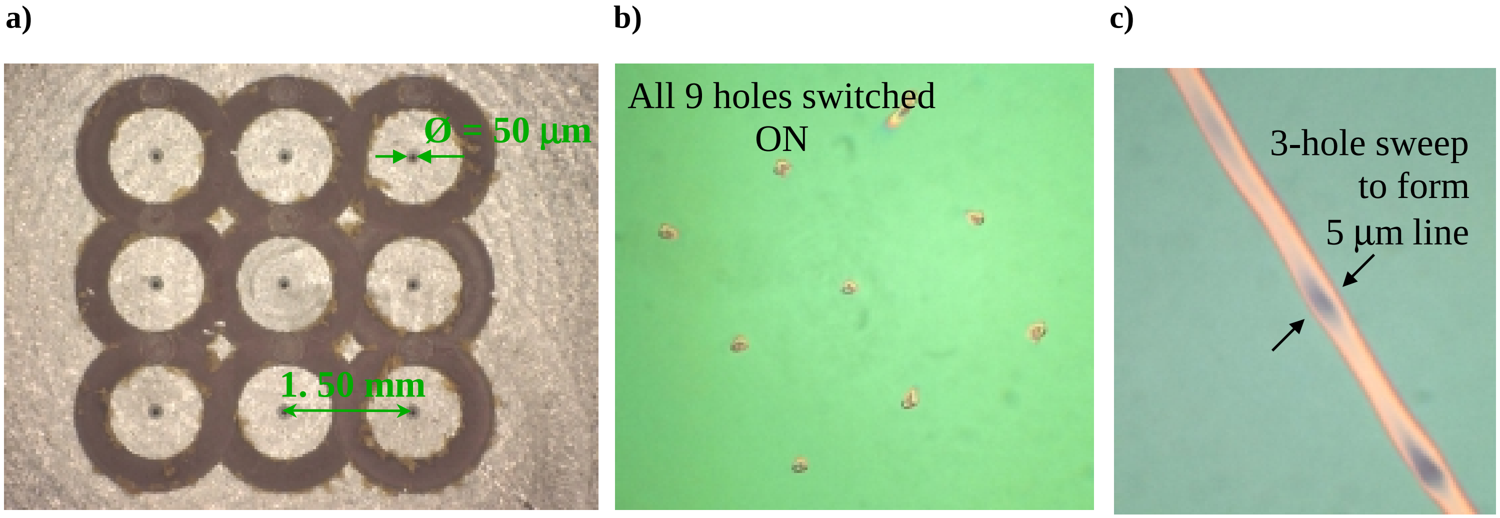
a)
Ø = 50 µm
1. 50 mm
b)
All 9 holes switched ON
c)
3-hole sweep to form 5 µm line

Figure 7:

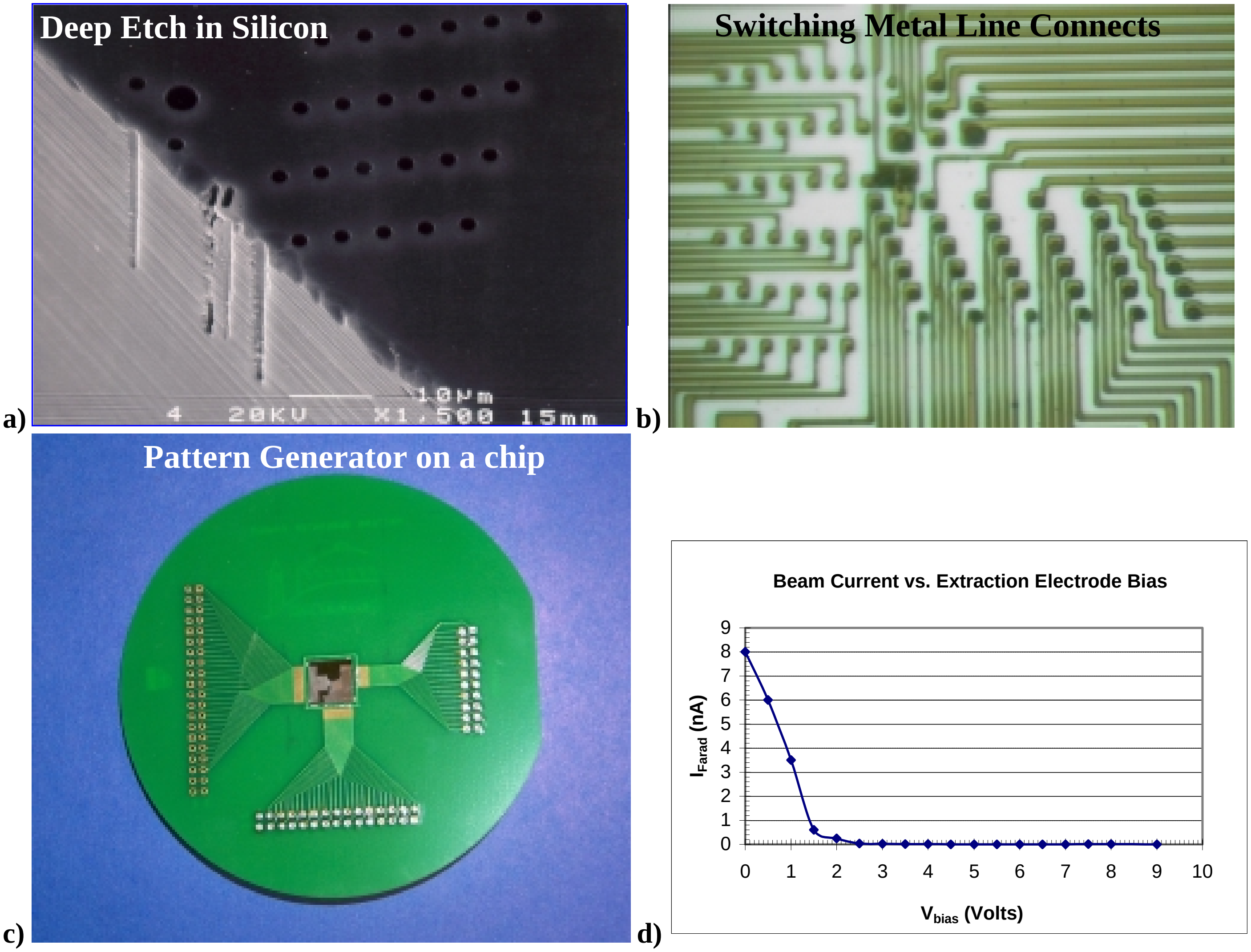
Deep Etch in Silicon
10μm
4 20KV X1,500 15mm
a)
Switching Metal Line Connects
b)
Pattern Generator on a chip
c)
Beam Current vs. Extraction Electrode Bias
I_{Farad} (nA)
9
8
7
6
5
4
3
2
1
0
0
1
2
3
4
5
6
7
8
9
10
V_{bias} (Volts)
d)

Figure 8:

a)

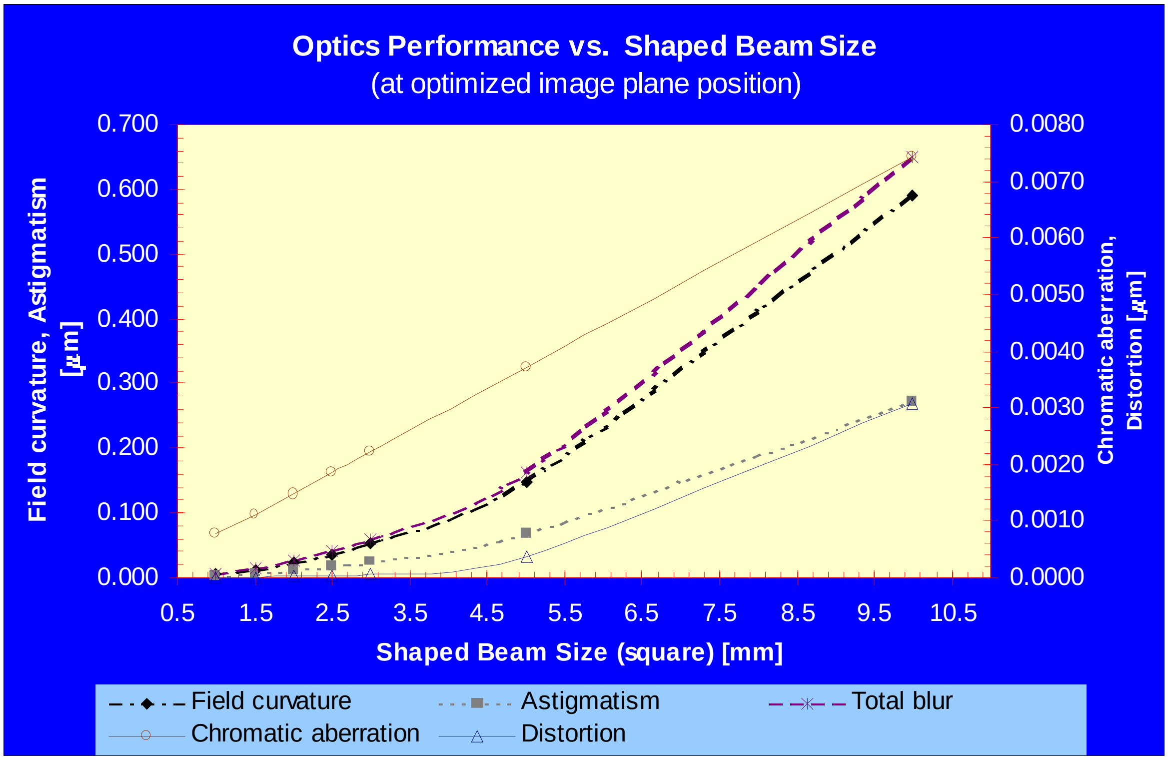

b)

IMS (IPL) Optics	Geometric Blur (nm)	Chromatic Blur (nm)	Stochastic Blur (nm)	Min. Total Blur (FWHM) (nm)	Total Permissible Blur (FWHM) (nm)
50 nm @ 2.2 µA (12.5x12.5 mm^2 subfield)	9	2.5	27	31	40
70 nm @ 3.2 µA (12.5x12.5 mm^2 subfield)	10	5	36	41	63
100nm @ 1.5µA (22x22 mm^2 subfield)	19	10	58	66	90

Figure 9:

a)

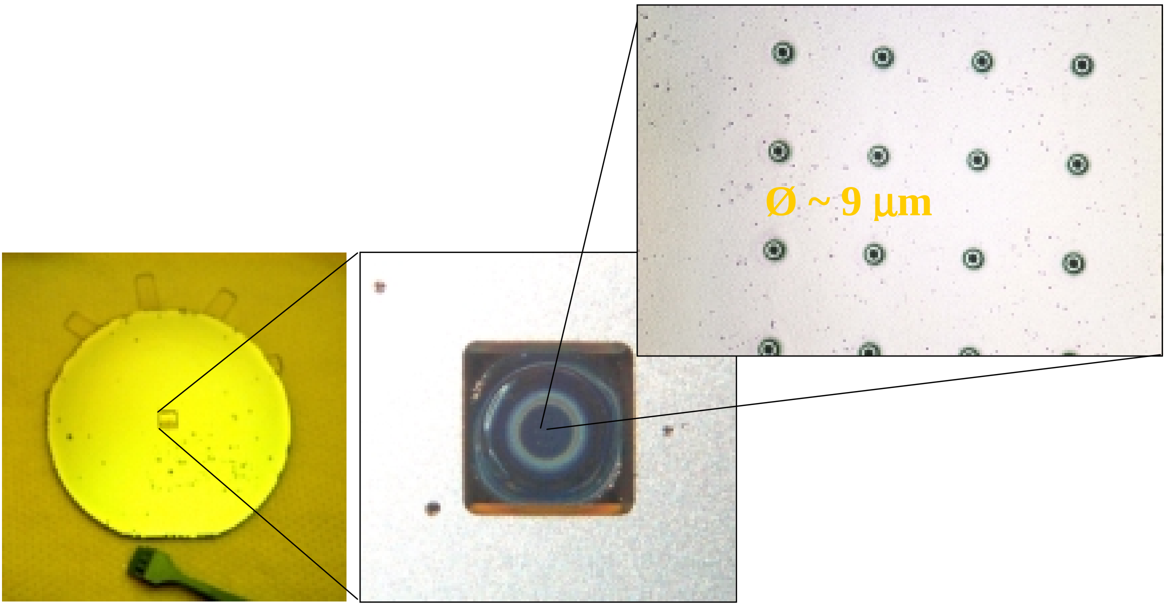

b)

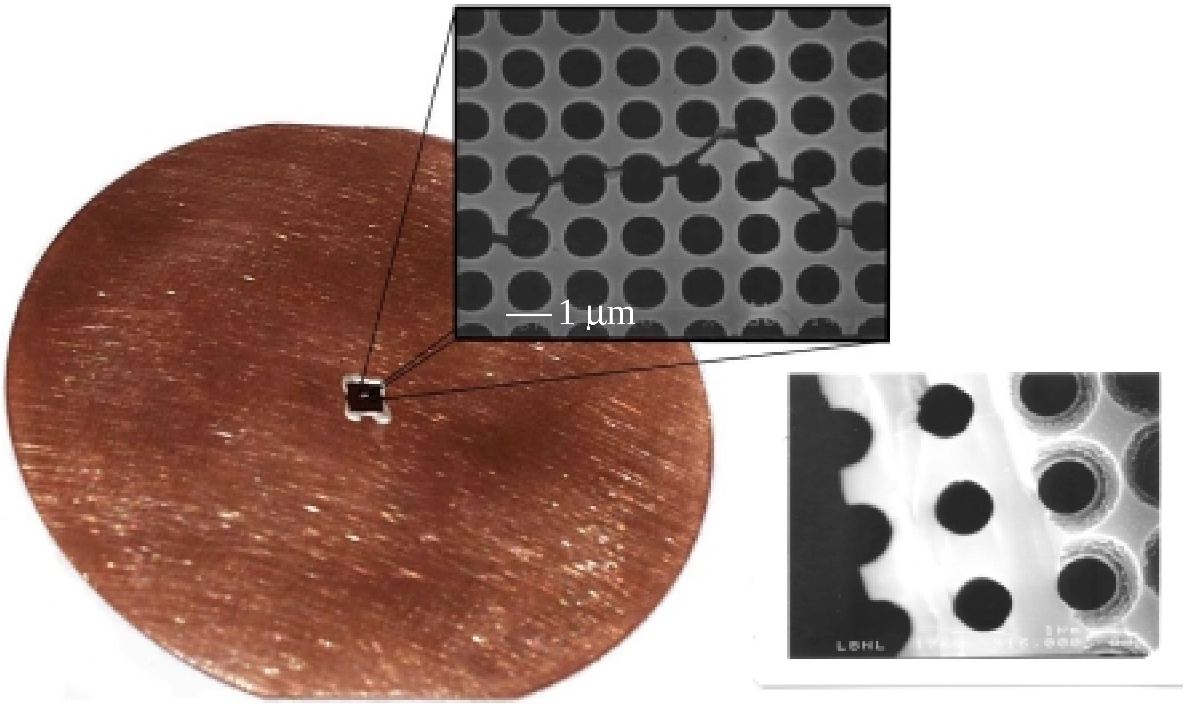

Figure 10:

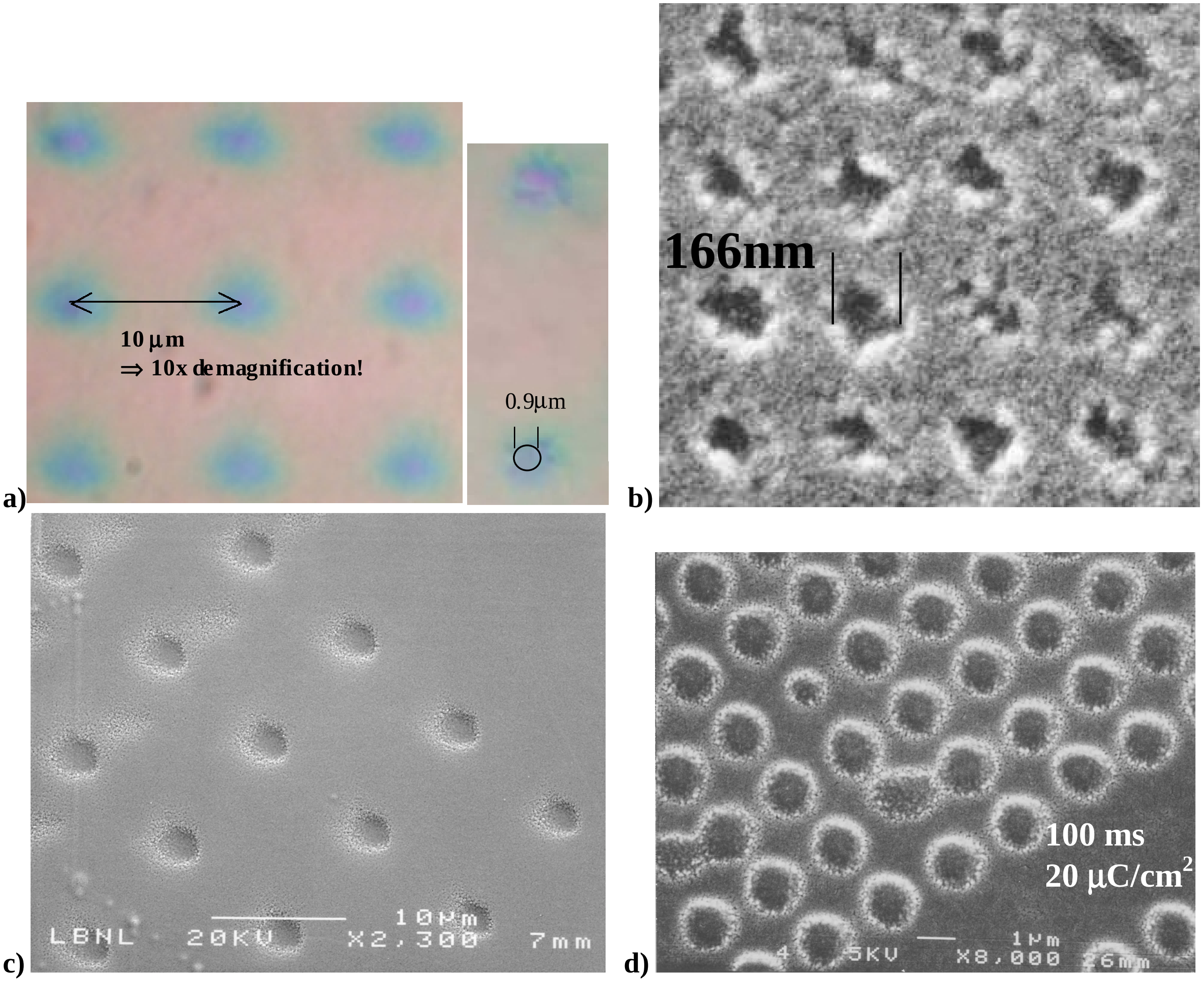
a)
10 µm
⇒ 10x demagnification!
0.9µm
b)
166nm
c)
LBNL 20KV X2,300 7mm
10µm
d)
100 ms
20 µC/cm²
5KV X8,000 26mm
1µm